Vortex-Induced Bending Oscillation of a Swept Wing

L. E. Ericsson*
Lockheed Missiles & Space Company, Inc., Sunnyvale, California

An analysis of existing experimental results shows that the observed bending oscillations of a highly swept wing cannot have been caused by the induced effects of a single leading-edge vortex, but rather by the interaction between two leading-edge vortices, one generated by a thick inner wing or wing/body glove and the other by the outboard, thin, variable-sweep wing. This inner/outer wing vortex interaction is similar to that occurring on a double-delta planform wing. The cause of the negative aerodynamic damping from the vortex interaction is the sensitivity to the angle of attack and its time derivative of the spanwise location of a leading-edge vortex.

Nomenclature

b = wing span
$\bar{c}$ = reference chord; mean aerodynamic chord
c = local wing chord (in streamwise direction)
g = damping; fraction of critical damping
ℓ = sectional lift; coefficient $c_\ell = 1/(\rho_\infty U_\infty^2/2)c$
M = Mach number
m = pitching moment; coefficient $C_m = m/(\rho_\infty U_\infty^2/2)Sc$
p = static pressure; coefficient $C_p = (p-p_\infty)/(\rho_\infty U_\infty^2/2)$
Re = Reynolds number, $= U_\infty \bar{c}/\nu_\infty$
S = reference area; projected wing area
s = local semispan
t = time
U = velocity
x = chordwise body-fixed coordinate
y = spanwise body-fixed coordinate; distance from symmetry plane of configuration
z = vertical body-fixed coordinate; distance above horizontal reference plane
α = reference angle of attack, in the streamwise direction
α_0 = local α for static wing loading
Δ = amplitude
θ = angular perturbation in pitch
Λ = leading-edge sweep
ν = kinematic viscosity of air
ρ = air density
ω = angular wing bending frequency

Subscripts

v = vortex
vb = vortex burst
∞ = freestream conditions

Differential Symbols

$\dot{\theta} = \partial\theta/\partial t$
$C_{m_{\dot{\theta}}} = \partial C_m/\partial(\bar{c}\dot{\theta}/U_\infty)$

Presented as Paper 86-1773 at the AIAA 4th Applied Aerodynamics Conference, San Diego, CA, June 9–11, 1986; received July 7, 1986; revision received Oct. 10, 1986.

*Senior Consulting Engineer. Fellow AIAA.

Introduction

THE swept-wing bending oscillation observed in flight as well as wind-tunnel tests[1] (Fig. 1) is but one example of a multitude of limit-cycle-type oscillations occurring on aircraft and aerospace vehicles.[2-13] The common prerequisites are 1) the aerodynamics are statically stabilizing, but dynamically destabilizing at small amplitudes and 2) the aerodynamics are highly nonlinear, with the total (aerodynamic plus structural or mechanical) damping changing from negative to positive when a certain amplitude is exceeded.

In the aircraft industry, stall flutter, i.e., torsional oscillations of a straight wing due to dynamic stall,[2-4] is a common phenomenon of general concern. In wind and/or marine engineering, it has its correspondence in the galloping phenomenon.[5-7] In the case of structural oscillations, structural damping aids in limiting the magnitude of the limit cycle type of oscillation.[8,9]

In the aerospace industry, blunt-nosed re-entry vehicles exhibit limit-cycling behavior due to separated flow effects[10] that result in decreased re-entry accuracy. For launch vehicles, on the other hand, the elastic oscillations that the structure can withstand are of very limited magnitude.[11-13] Fortunately, structural damping can often save the structure. Its magnitude relative to the aerodynamic (negative) damping is substantial in the case of bodies of revolution, but is relatively insignificant for an aircraft wing.

It is worth noting that in spite of the general sameness of the oscillatory character, the fluid mechanical cause of the self-induced oscillations can be very different. It will be shown that the present wing bending oscillations are caused by leading-edge-vortex interactions, with the resulting unsteady aerodynamics closely related to those for slender delta wings.[14,15]

Swept-Wing Aerodynamics

The variation of aerodynamic damping with angle of attack and sweep angle[1] (Fig. 2) shows that, at 55- and 25-deg sweep, shock/boundary-layer interaction causes the expected increase of the damping.[16] However, the damping characteristics at 67.5- and 65-deg sweep are very different and look like those generated on a straight wing by "sudden separation" effects,[16,17] except that in the swept-wing case the extreme Mach sensitivity of the straight wing[16,17] is absent (Fig. 3). The symbols designate different air densities and, hence, different Reynolds numbers. Within the data accuracy, no consistent Reynolds number trend can be distinguished. The data in Fig. 3 designate the lowest angle of attack for which the self-excited oscillation was observed.

The α range for the oscillation was extremely narrow (Fig. 2), in no case exceeding 1 deg. The characteristics shown in Fig. 3 rule out shock-induced flow separation as a source of the self-excited oscillation, as was also concluded in Ref. 1, where it was suggested that one or both of the following vortex-induced effects was the source.

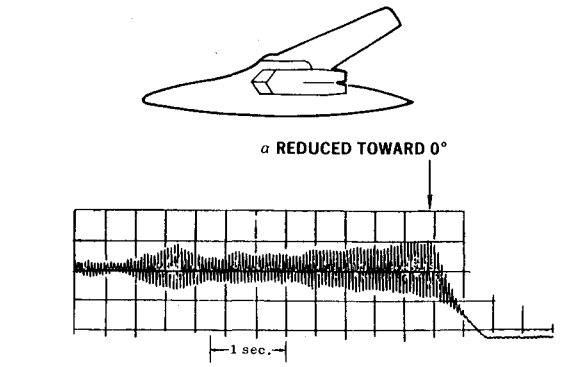

SWEEP ANGLE, DEG	α_{FUSE} DEG	MACH NUMBER	REYNOLD'S NUMBER	TIP AMPLITUDE IN.
67.5	7.36	0.975	5.9×10^6	±0.76

Fig. 1 Self-excited wing bending strange gage response (from Ref. 1).

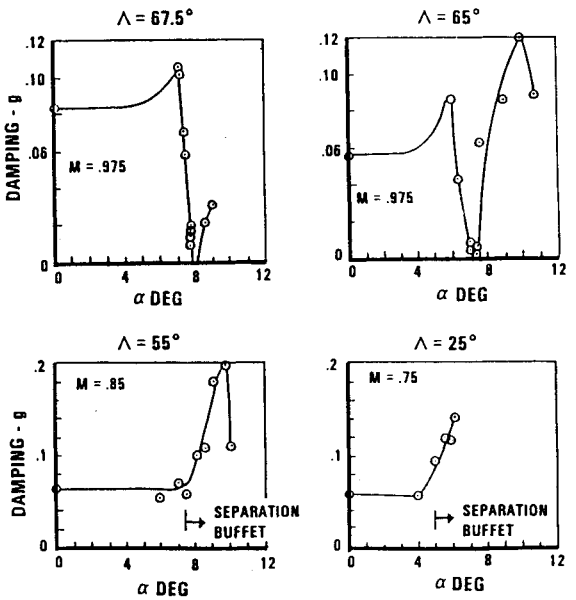

Fig. 2 Measured damping of first bending mode (from Ref. 1).

Figure 4 shows the two suggested flow mechanisms. In one case (left diagram), the suggested source is the changing strength of the leading-edge vortex with increasing angle of attack, which due to the phase lag can generate a dynamically destabilizing lift component. The mechanism would be similar to that for the "spilled" leading-edge vortex in dynamic airfoil stall.[4] This suggested mechanism has one big flaw: the effect is not limited to one narrow angle-of-attack region, but should instead increase with increasing α. In the other case (right diagram), the suggested mechanism is the breakdown of the leading-edge vortex. This would have a

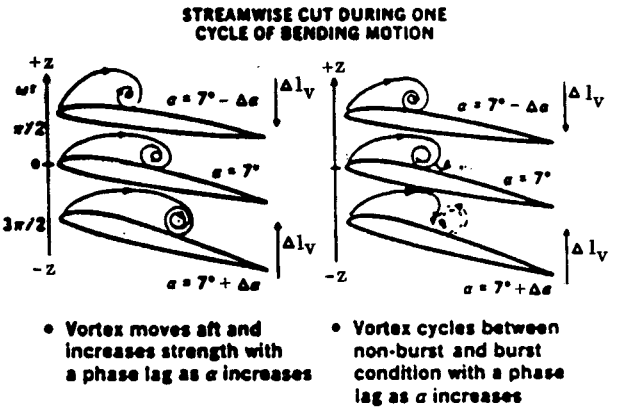

Fig. 4 Two possible mechanisms for self-excited oscillations (from Ref. 1).

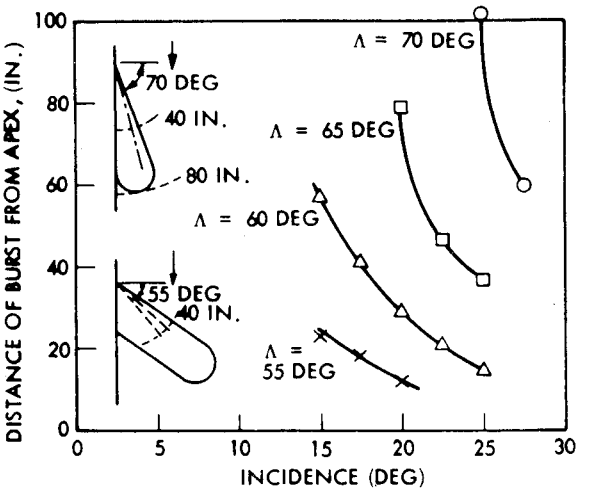

Fig. 5 Vortex burst as a function of sweep and angle of attack (from Ref. 18).

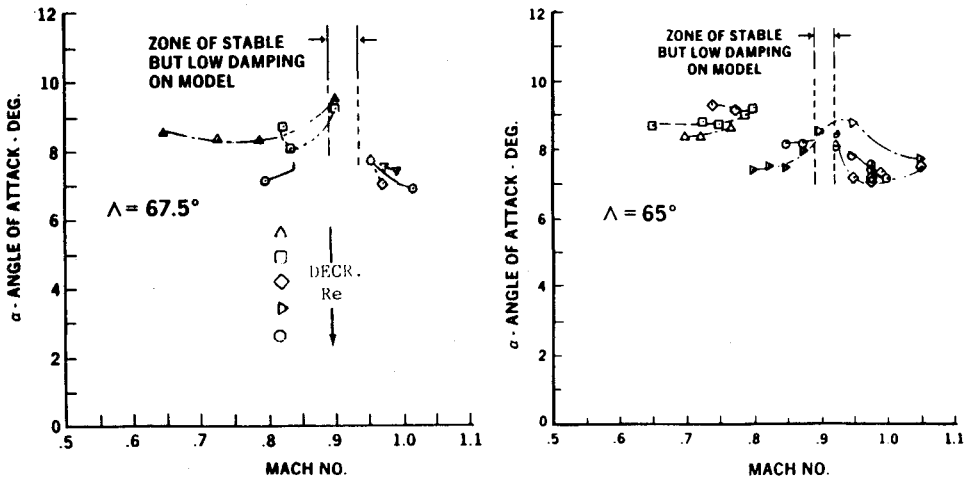

Fig. 3 Angle of attack for starting self-excited oscillations (from Ref. 1).

critical angle of attack associated with it. However, this angle would be well beyond $\alpha = 7$ deg according to the results obtained by Lambourne and Bryer[18] (Fig. 5). One additional requirement would have been a phase lag 180 deg larger than in the first case (left diagram), as vortex burst causes a loss of lift.

Thus, none of the suggested flow mechanisms can have caused the observed self-excited bending oscillations of the swept wing. The present author agrees with the conclusion drawn in Ref. 1—that the oscillations are vortex induced. However, the source is not a single leading-edge vortex, but rather the interaction between two leading-edge vortices.†

Analysis

The photograph of the model[1] (Fig. 6) shows that the variable-sweep, thin outboard wing is preceded by a fixed-sweep (67.5 deg) thick inboard wing or glove. The difference in leading-edge radii is illustrated further by the cross-sectional diagram in Fig. 7. Even for the same leading-edge sweep angle, the inner and outer wings will start generating leading-edge vortices at different angles of attack because of the difference in their leading-edge roundness.[19] Using the stall angles for 12 and 9% thick airfoils[20] (Fig. 8) to represent the inner and outer wings, respectively, one finds that for 67.5-deg leading-edge sweep the respective wings should start developing leading-edge vortices at 6.3 and 4.5 deg. Compressibility-induced apparent sharpening of the leading edge could probably make the very thick inner wing glove (Fig. 7) act as a 12% thick airfoil in incompressible flow, whereas the leading edge of the outer wing becomes practically sharp, causing vortex development to start at $\alpha > 0$. Thus, considering that the inner vortex must gain some strength before it can interact with the outer wing vortex, one can see how the critical α value shown in Fig. 3 can result. That leading-edge roundness does delay the generation of a leading-edge vortex in the manner described in Ref. 19 has been shown by comparison with experimental results[21] (Fig. 9.) The vortex-induced effects do not occur until $\alpha > 5$ deg.

When the inner wing starts developing a leading-edge vortex, it will trail inboard of the already existing leading-edge vortex on the outer wing. That is, the situation is similar to the one existing for a double-delta wing[22] (Fig. 10). Figure 10 shows how the oil flow visualization results are correlated with the position of the (primary) leading-edge vortices from outer and inner delta-wing leading edges. The measured suction peaks indicate the locations of the vortices. When the angle of attack is increased above a certain critical value, the outer and inner leading-edge vortices start to interact with each other, as illustrated by the oil flow photographs[23] in Fig. 11 and the smoke flow visualizations[24] in Fig. 12. In Fig. 11a, at $\alpha = 5$ deg, the two vortices are separate, as in Fig. 10. At $\alpha = 7$ deg, however, the two vortices have started to interact (Fig. 11b) and, at $\alpha = 10$ deg (Fig. 11c), they have combined into one vortex. The smoke flow photograph in Fig. 12 shows the interaction between the two vortices.

When one compares the flow visualization pictures for the double-delta wing planform (Figs. 11 and 12) with the oil flow visualization for the swept wing[1] (Fig. 13), one can see certain similarities. However, a more direct comparison, quantitative rather than qualitative, can be made by comparing the experimental pressure distributions for the double-delta planform[23] (Fig. 14) and the swept wing[1] (Fig. 15). Figure 14 shows that the inner delta wing vortex when it interacts with the vortex on the outer wing, causes the sectional loading to increase and shift its center inboard. Noticing that the spanwise inboard movement on the delta wing[23] (Fig. 14) corresponds to a chordwise aft movement on the swept wing[1] (Fig. 15), one can conclude that the inner/outer vortex interactions do indeed cause very similar changes in the load distributions. The oscillation occurred when the load distribution in Fig. 15 changed from that typical for a single leading-edge vortex ($\alpha = 6.9$ deg) to that typical for the two-vortex interaction discussed earlier ($\alpha = 8$ deg).

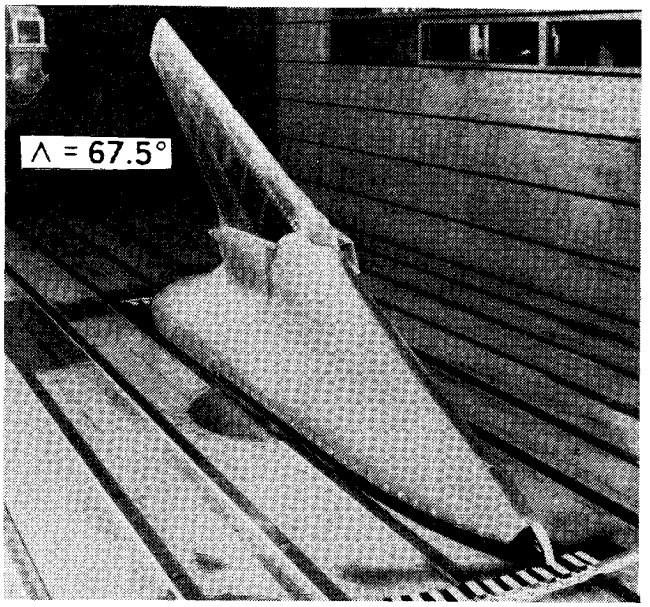

Fig. 6 Model mounted in NASA Ames 11-ft Transonic Wind Tunnel (from Ref. 1).

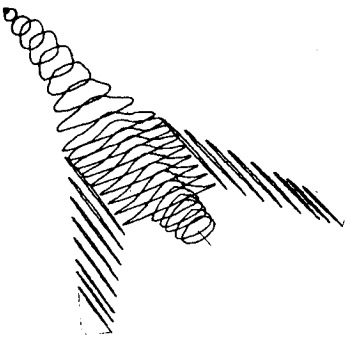

Fig. 7 Graph of wing and body cross sections (courtesy of Steve Dobbs).

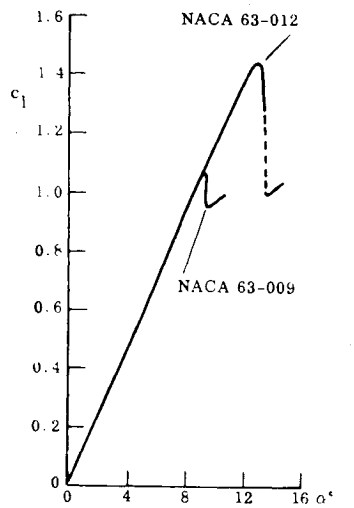

Fig. 8 Effect of airfoil thickness on maximum lift (from Ref. 20).

†As was suggested by Atlee Cunningham when Ref. 1 was presented in April 1985.

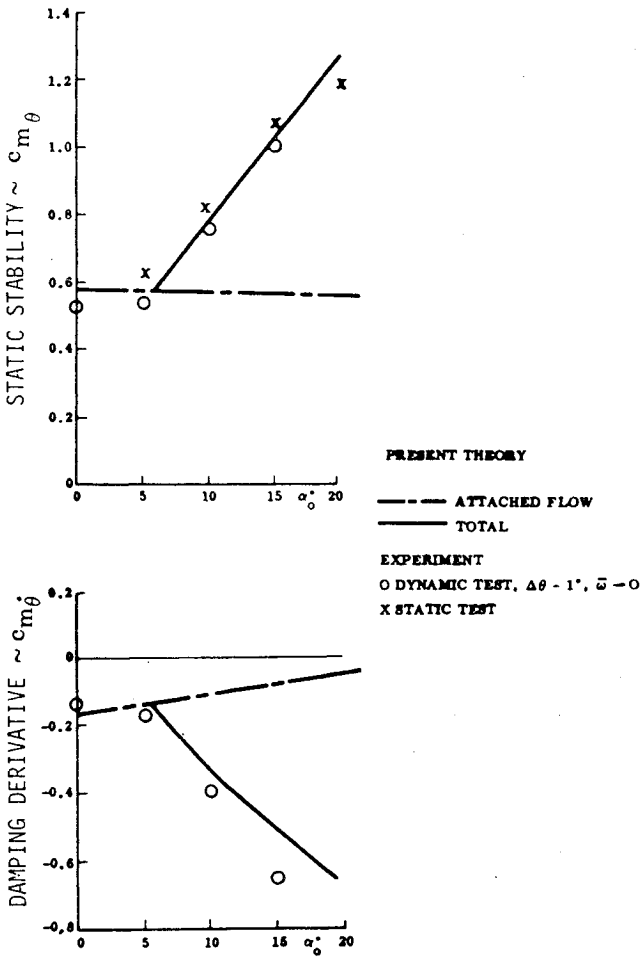

Fig. 9 Effect of leading-edge roundness on delta-wing aerodynamics (from Ref. 19).

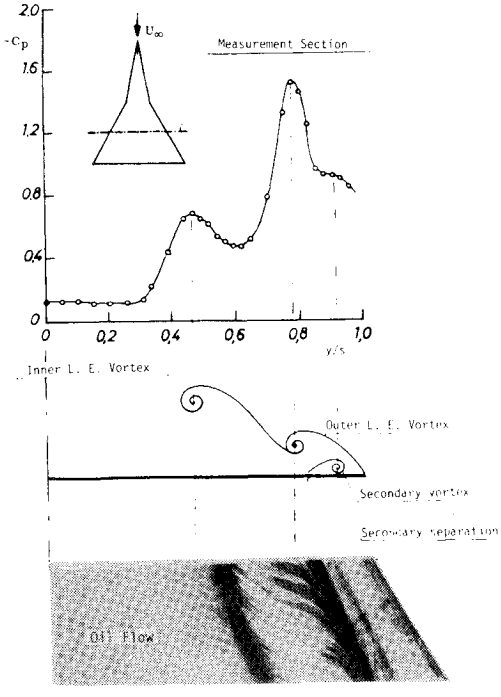

Fig. 10 Inner and outer leading-edge vortices on a double-delta wing at $\alpha = 12$ deg (from Ref. 22).

The interaction between inner and outer wing vortices described above fits the experimental facts in regard to the observed bending oscillation of the swept wing[1] (Fig. 2). Thus, it produces a critical α range in which the single-vortex loading is being transformed to that resulting from the two interacting vortices. At higher angles of attack, the two vortices are merged into one and no self-excited bending oscillation will result. Furthermore, the large-amplitude pressure oscillations are localized to the wing region where one expects the two-vortex interaction to take place[1] (Fig. 16).

Unsteady Aerodynamics

Figure 17 shows the spanwise variation of the local, streamwise angle of attack for $\Lambda = 67.5$ deg and a fuselage angle of attack of $\alpha = 7.38$ deg. The solid line shows the variation due to static loads and the dash-dot lines the extreme values $\alpha_0 + \Delta\alpha$ and $\alpha_0 - \Delta\alpha$ during the down- and upstroke portions of the bending oscillations. The inner thick wing glove is at the constant angle of attack α_0. Consequently,

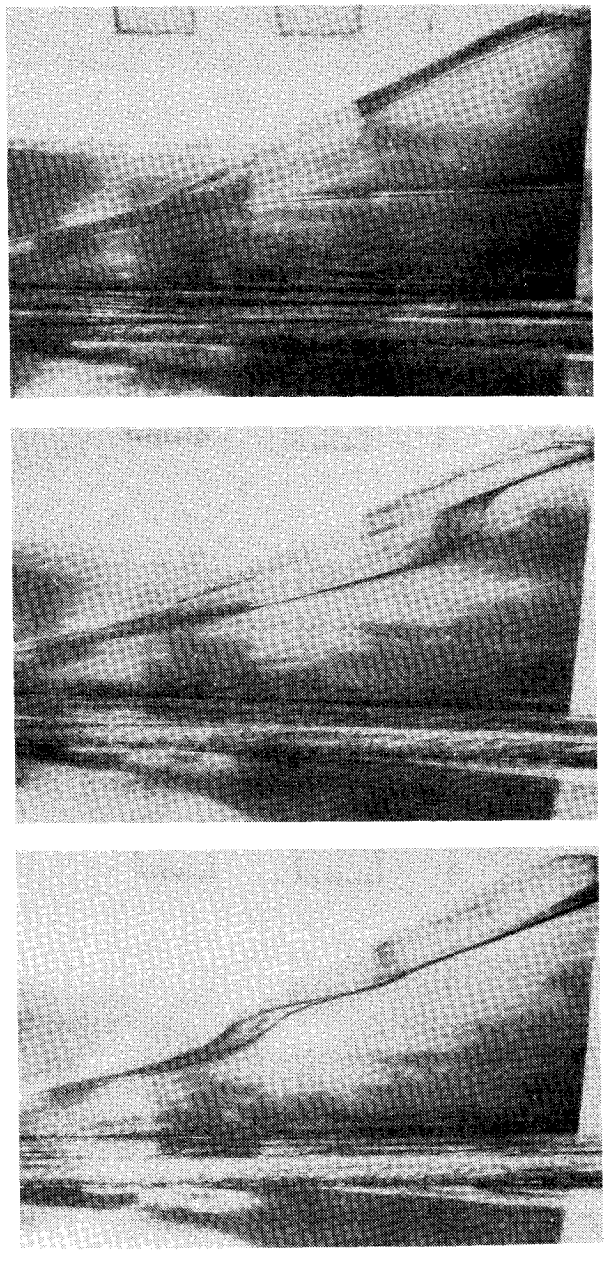

Fig. 11 Oil flow visualization of inner/outer leading-edge vortex interaction on a 75/62-deg double-delta wing (from Ref. 23): a) $\alpha = 5$ deg, b) $\alpha = 7$ deg, c) $\alpha = 10$ deg.

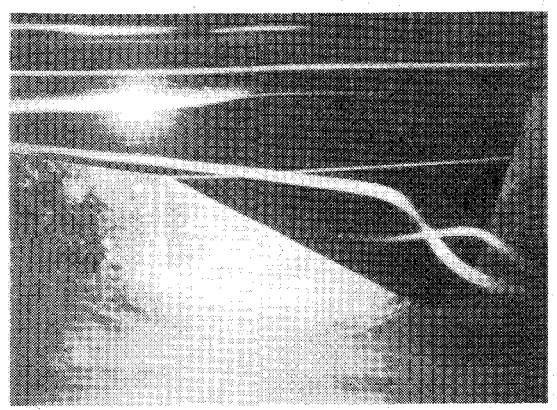

a)

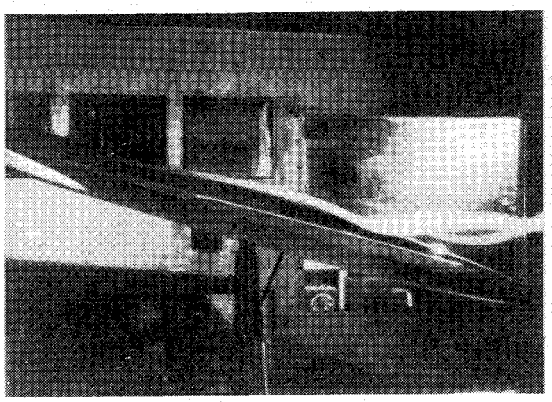

b)

Fig. 12 Smoke flow visualization of inner/outer leading-edge vortex interaction on a 77.2/59-deg double-delta wing at $\alpha = 16$ deg (from Ref. 24): a) plan view, b) side view.

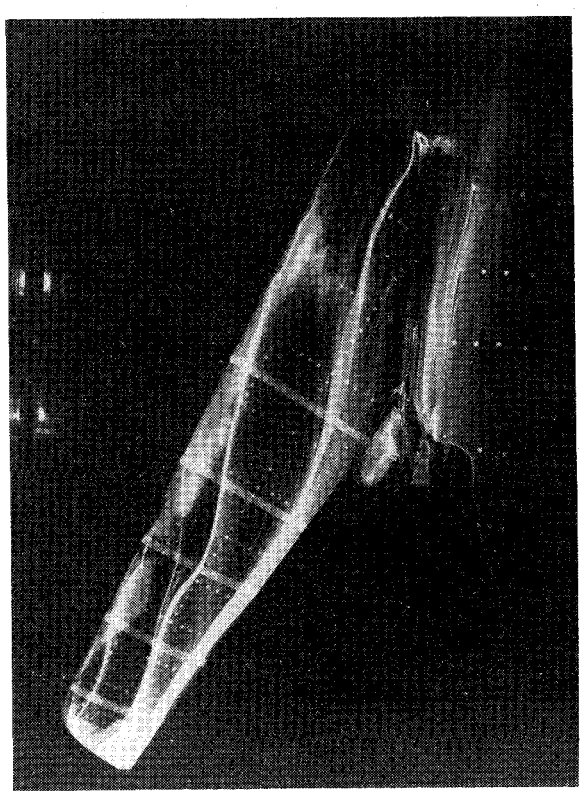

Fig. 13 Oil flow visualization of swept-wing flow (from Ref. 1).

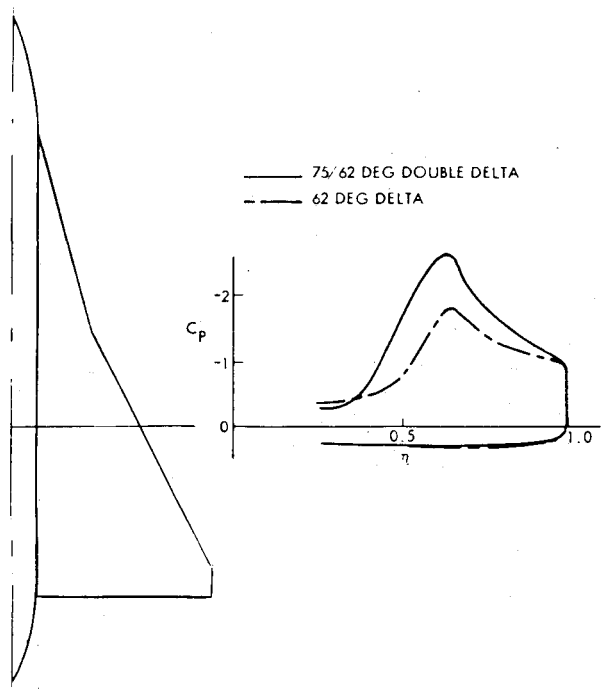

Fig. 14 Vortex-induced loads on a 75/62-deg double-delta wing at $\alpha = 20$ deg (from Ref. 23).

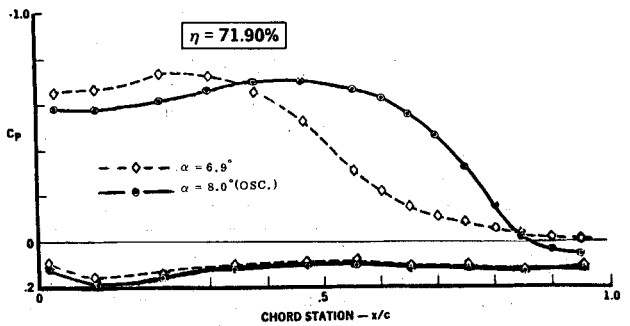

Fig. 15 Static pressure distribution at $M_\infty = 0.80$ on 65-deg swept wing.

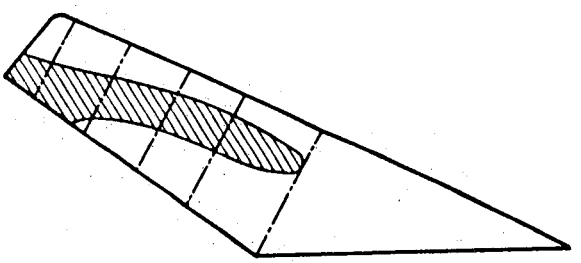

Fig. 16 Zone of large-amplitude unsteady pressures on 67.5-deg swept wing at $M_\infty = 0.975$ and $\alpha = 7.4$ deg (from Ref. 1).

the effective apex of the outer wing does not move and the only effect of the leading-edge vortex is the entrainment enhancement of the attached flow loads.[14] If one approximates the α_0 curve in Fig. 17 with a straight line, one can apply the analysis method of Ref. 14 directly. In any case, the single leading-edge vortex will increase the damping in pitch for the rigid delta wing and the damping in bending for the present swept wing at a rate proportional to $\sin\alpha$. This is essentially the single-vortex data trend exhibited in Fig. 2. The deviation is the interaction at $7 < \alpha < 9$ deg between the inner and outer vortices. It is also likely to be minor variations in the shock/boundary-layer interaction.[16] Thus, what

remains to be described is how the vortex interaction at $7<\alpha<9$ deg can cause negative aerodynamic damping. [Although the interaction is likely to generate a forcing function (buffet) due to general flow unsteadiness, the large-amplitude response is caused by negative aerodynamic damping.]

Whereas the single-vortex effect is almost exclusively due to changing vortex strength, at least in regard to longitudinal aerodynamics such as the pitch damping for a delta wing[14] or the damping in bending for the present swept wing, in the case of the outer/inner vortex interaction, the spanwise movement of the leading-edge vortex on the outer wing becomes important. It has been shown by Randall[25] that the leading-edge vortex describes spanwise oscillations around its static position (Fig. 18). Thus, during the α-increasing part of the pitch oscillation, the vortex is outboard of its static position and, during the α-decreasing part, it is inboard. The spanwise location of the leading-edge vortex for a stepwise changing angle of attack and its static position is shown in Fig. 19 for a very slender delta wing.[26] (For a less slender wing, i.e., with less leading-edge sweep, the vortex will not be as far inboard.) The figure shows that for the moderate angle-of-attack range of interest in the present case, the spanwise location of the vortex is very sensitive to the angle of attack. This explains the narrow α range for outer/inner vortex interaction of the present swept wing.

With the aid of Figs. 15, 17, and 18, one can see how, when the wing angle of attack is increasing, the load distribution will change toward the front-loaded one for the undisturbed wing leading-edge vortex. Conversely, the change will be toward the aft-loaded one, generated by the interaction from the glove vortex, when the angle of attack is decreasing. Figure 17 shows that the streamwise angle of attack of the swept wing is decreasing during the bending upstroke, $0<\omega t<\pi$, and increasing during the bending downstroke, $\pi<\omega t<2\pi$, with the extreme values reached at $\omega t=\pi/2$ and $3\pi/2$, respectively. Because the apex of the outer-wing leading edge is not moving, the phase lages involved will be small. Consequently, the load distribution extremes will occur close to $\omega t=\pi/2$ and $3\pi/2$. This is illustrated by the results in Fig. 20. Thus, during the bending upstroke, the lift is increased and thereby the bending moment, whereas during the downstroke, lift and bending moment are decreased by the vortex interaction. In both cases, the dynamic effect is destabilizing, driving the bending oscillations, which is in agreement with the experimental results.[1] (Note that a delta wing is less likely to develop such bending oscillations due to its different structural characteristics.)

Although the analysis in Ref. 14 can be modified and extended to apply to the bending oscillations of a swept wing, the practical interest is in eliminating the bending oscillation, not in predicting its amplitude characteristics. Generally, one would have the usual scaling problems and would have to use analytic extrapolation to predict the full-scale dynamic characteristics.[27,28]

The fixes tried to eliminate the bending oscillation[1] (Fig. 21) were all addressing the outer-wing flow, aimed at stopping possible adverse shock/boundary-layer interaction. Of all the fixes tested, only the inboard fence could have affected the outer/inner vortex interaction, possibly causing the inner wing/body glove to burst. However, if the spiral burst, observed on delta wings,[18] occurred, the result may be only to move the interaction to another α range due to the enlarged size and changed character of the inner vortex. One would expect that if the leading-edge stall strip had been placed on the inner wing or wing/body glove, both the inner and outer wing vortices would have started to develop at the same time (same α) for the same leading-edge sweep, resulting in a single leading-edge vortex, thereby possibly eliminating the bending oscillations. (It would at least have moved the interaction down to lower angles of attack, where the vortex-induced loads would be much smaller.)

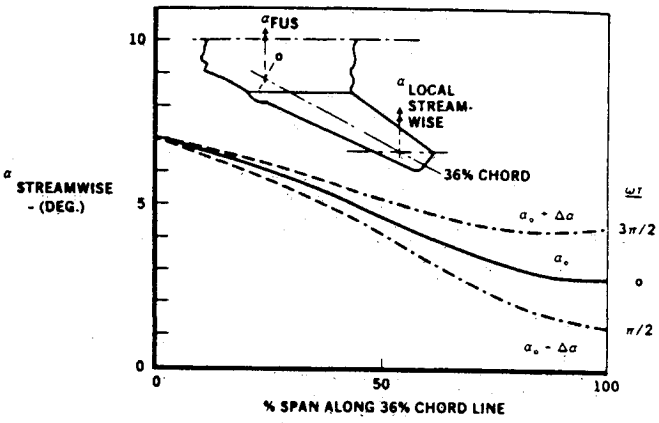

Fig. 17 Streamwise angle-of-attack variation during limit cycle oscillation of 67.5-deg swept wing at $M_\infty=0.975$ and $\alpha=7.38$ deg (from Ref. 1).

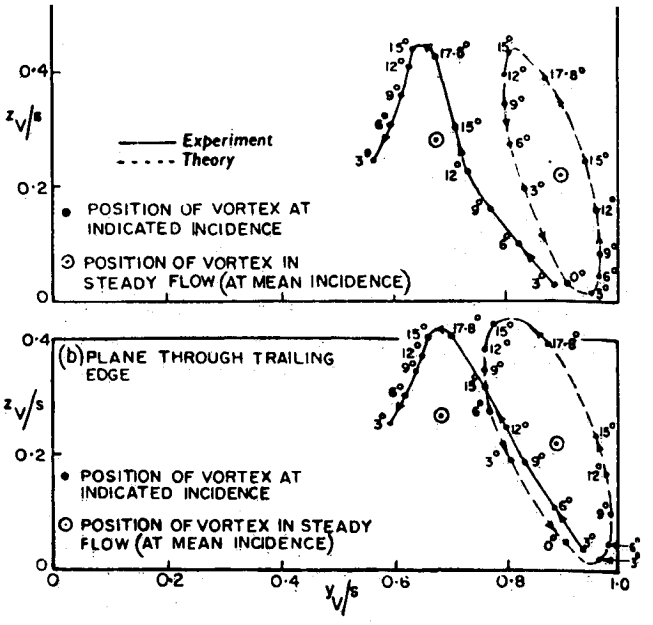

Fig. 18 Leading-edge vortex movement during pitch oscillation of a slender delta wing (from Ref. 25).

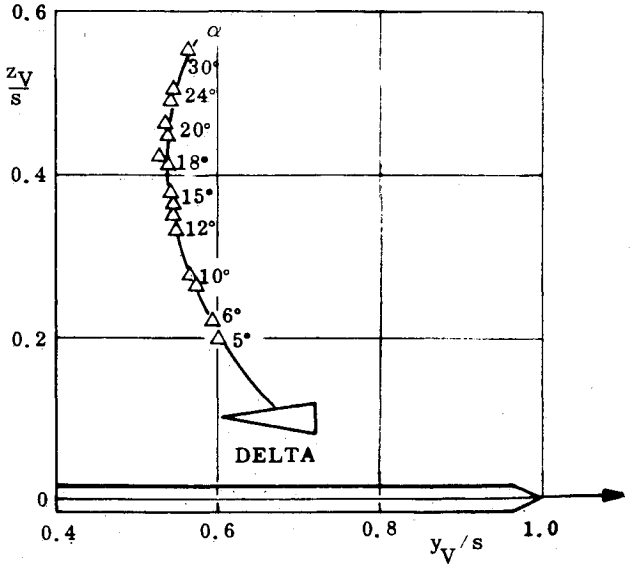

Fig. 19 Spanwise vortex movement on a slender delta wing as a function of angle of attack (from Ref. 26).

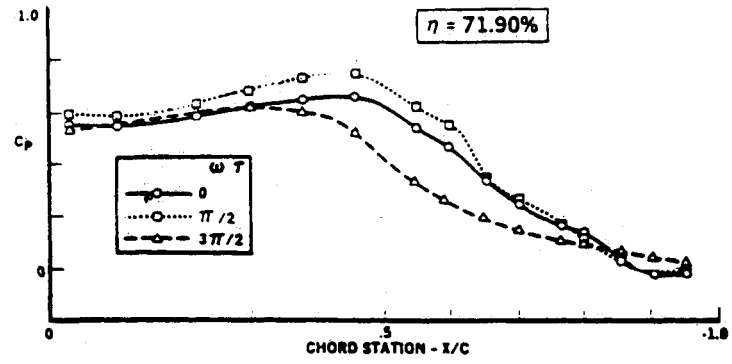

Fig. 20 Upper surface pressure distribution for the extreme positions of the bending motion of 65-deg swept wing at $M_\infty = 0.80$ and $\alpha = 7.44$ deg (from Ref. 1).

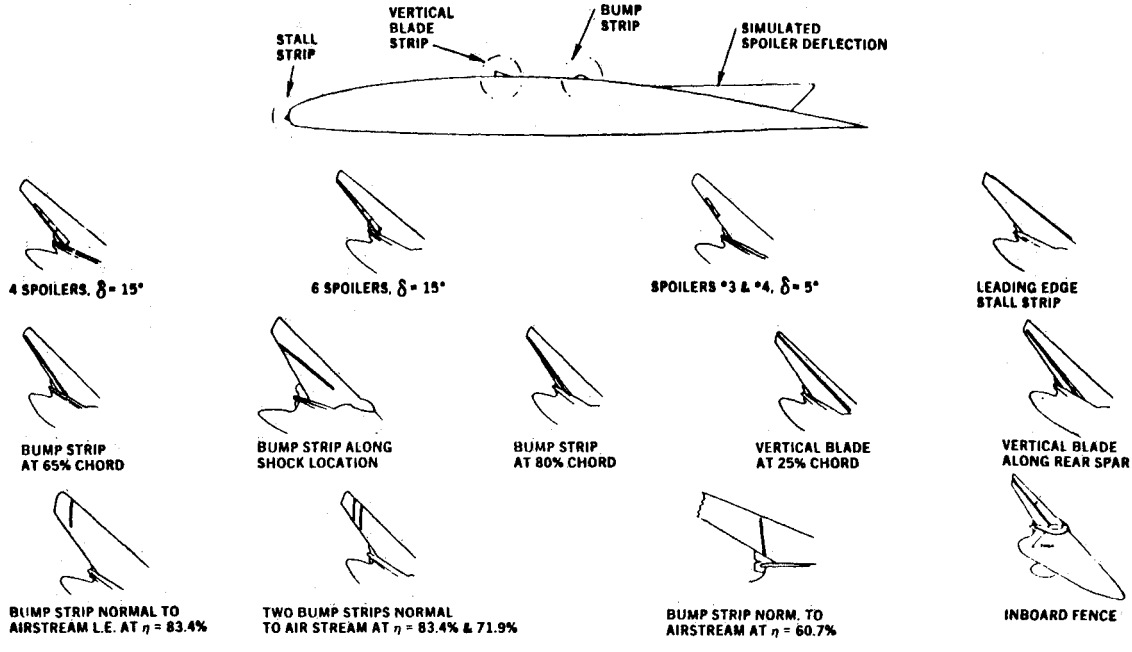

Fig. 21 Aerodynamic fixes tested (from Ref. 1).

Conclusions

An analysis of available experimental results in regard to the observed bending oscillation of a swept wing has led to the following conclusions:

1) The bending oscillations occur only within a very narrow angle-of-attack range and can, therefore, not be caused by the induced effects of a single leading-edge vortex, with or without the occurrence of vortex burst.

2) The bending oscillations are instead caused by the interaction between two leading-edge vortices, one from the thin outer wing and one from the inner thick wing glove. The leading-edge vortex will develop later (at a higher angle of attack), on the inner wing than on the outer wing, and the interaction is similar to the one expected for a double-delta wing geometry.

The undamping effect of the vortex interaction results because of the sensitivity of the spanwise location of a leading-edge vortex to not only the streamwise angle of attack, but also to the magnitude and direction of the angular rate.

Acknowledgment

The author is indebted to Atlee Cunningham Jr. and Steven Dobbs for obtaining the detailed information about the observed phenomena and to Nancy Behney for her help with the manuscript.

References

[1]Dobbs, S. K., Miller, G. D., and Stevenson, J. R., "Self-Induced Oscillation Wind Tunnel Test of a Variable Sweep Wing," AIAA Paper 85-0739, April 1985.

[2]Ericsson, L. E. and Reding, J. P., "Stall Flutter Analysis," *Journal of Aircraft*, Vol. 10, Jan. 1973, pp. 5–13.

[3]Ericsson, L. E. and Reding, J. P., "Dynamic Stall Analysis in Light of Recent Numerical and Experimental Results," *Journal of Aircraft*, Vol. 13, April 1976, pp. 248–255.

[4]Ericsson, L. E. and Reding, J. P., "Dynamic Stall At High Frequency and Large Amplitude," *Journal of Aircraft*, Vol. 17, March 1980, pp. 136–142.

[5]Ericsson, L. E. and Reding, J. P., "Potential Hydroelastic Instability of Profiled Underwater Structures," *Journal of Hydronautics*, Vol. 14, Oct.–Dec. 1980, pp. 97–104.

[6]Ericsson, L. E., "Hydroelastic Effects of Separated Flow," *AIAA Journal*, Vol. 21, March 1983, pp. 452–458.

[7]Ericsson, L. E., "Limit Amplitude of Galloping Bluff Cylinders," *AIAA Journal*, Vol. 22, April 1984, pp. 493–497.

[8]Ericsson, L. E. and Reding, J. P., "Aeroelastic Characteristics of the Space Shuttle External Tank Cable Trays," *Journal of Spacecraft and Rockets*, Vol. 22, May–June 1985, pp. 289–296.

[9]Ericsson, L. E., "Engineering Approximation of Beam Flutter," *Journal of Spacecraft and Rockets,* Vol. 21, Jan.–Feb. 1984, pp. 6–8.

[10]Ericsson, L. E., "Unsteady Aerodynamics of Separating and Reattaching Flow on Bodies of Revolution," Vol. 1, *Recent Research on Unsteady Boundary Layers, IUTAM Symposium,* Laval University, Quebec, Canada, May 1971, pp. 481–512.

[11]Ericsson, L. E., "Aeroelasticity, Including Dynamic Effects of Separated Flow," AGARD LS-114, March 1981, Lecture 13.

[12]Ericsson, L. E. and Reding, J. P., "Analysis of Flow Separation Effects on the Dynamics of a Large Space Booster," *Journal of Spacecraft and Rockets,* Vol. 2, July–Aug. 1965, pp. 481–490.

[13]Ericsson, L. E., "Aeroelastic Instability Caused by Slender Payloads," *Journal of Spacecraft and Rockets,* Vol. 4, Jan. 1967, pp. 65-73.

[14]Ericsson, L. E. and Reding, J. P., "Unsteady Aerodynamics of Slender Delta Wings at Large Angles of Attack," *Journal of Aircraft,* Vol. 12, Sept. 1975, pp. 721–729.

[15]Ericsson, L. E., "The Fluid Mechanics of Slender Wing Rock," *Journal of Aircraft,* Vol. 21, May 1984, pp. 322–328.

[16]Ericsson, L. E., "Dynamic Effects of Shock-Induced Flow Separation," *Journal of Aircraft,* Vol. 12, Feb. 1975, pp. 86–92 (Errata, *Jounal of Aircraft,* Vol. 18, July 1981, p. 608).

[17]Erickson, L. L., Gambucci, B. J., and Wilcox, P. R., "Effects of Space Shuttle Configuration on Wing Buffet and Flutter, Part II: Thick High Aspect Ratio Wing," *NASA Space Shuttle Technology Conference, Dynamics and Aeroelasticity,* NASA TMX-2274, Vol. III, 1971, pp. 209–229.

[18]Lambourne, N. C. and Bryer, D. W., "The Bursting of Leading-Edge Vortices—Some Observations and Discussion of the Phenomenon," British Aeronautical Research Council, R&M 3282, 1962.

[19]Ericsson, L. E. and Reding, J. P., "Approximate Nonlinear Slender Wing Analysis," *Journal of Aircraft,* Vol. 14, Dec. 1977, pp. 1197–1204.

[20]McCullough, G. B. and Gault, D. E., "Examples of Three Representative Types of Airfoil-Section Stall at Low Speed," NACA TN 2502, 1951.

[21]Woodgate, L., "Measurements of the Oscillatory Pitching Moment Derivatives on a Delta Wing with Rounded Leading Edges in Incompressible Flow," British Aeronautical Research Council, R&M 3628, Pt. 1, July 1968.

[22]Krogmann, P., "Experimentelle und Theoretische Untersuchungen an Doppeldeltaflügeln, Aerodynamische Versuchsanstalt, Göttingen, FRG, Bericht 68A35," July 1968.

[23]Wendtz, W. H. Jr. and McMahon, M. C., "An Experimental Investigation of the Flow Fields About Delta and Double-Delta Wings at Low Speeds," NASA CR-521, Aug. 1966.

[24]Sacks, A. H., Lundberg, R. E., and Hanson, C. W., "A Theoretical Investigation of the Aerodynamics of Slender Wing-Body Combinations Exhibiting Leading-Edge Separation," NASA CR-719, March 1967.

[25]Randall, D. G., "Oscillating Slender Wings with Leading-Edge Separation," *The Aeronautical Quarterly,* Vol. XVII, Nov. 1966, pp. 311–331.

[26]Werlé, H., "Vortices from Very Slender Wings," *La Rechérche Aerospatiale,* No. 109, Nov.–Dec. 1965, pp. 1–12.

[27]Ericsson, L. E. and Reding, J. P., "Analytic Extrapolation to Full Scale Aircraft Dynamics," *Journal of Aircraft,* Vol. 21, March 1984, pp. 222-224.

[28]Ericsson, L. E. and Reding, J. P., "Dynamic Simulation Through Analytic Extrapolation," *Journal of Spacecraft and Rockets,* Vol. 19, March–April 1982, pp. 160–166.